Brain Struct Funct (2015) 220:27–36
DOI 10.1007/s00429-013-0633-4

ORIGINAL ARTICLE

Experimental focal neocortical epilepsy is associated with reduced white matter volume growth: results from multiparametric MRI analysis

Willem M. Otte · Maurits P. A. van Meer · Kajo van der Marel · René Zwartbol · Max A. Viergever · Kees P. J. Braun · Rick M. Dijkhuizen

Received: 22 February 2013 / Accepted: 30 August 2013 / Published online: 8 September 2013

Abstract Focal epilepsy has recently been associated with remote white matter damage, including reduced white matter volume. Longitudinal assessment of these white matter changes, in relation to functional mechanisms and consequences, may be ideally done by in vivo neuroimaging in well-controlled experimental animal models. We assessed whether advanced machine learning algorithm models could accurately detect volumetric changes in white matter from multiparametric MR images, longitudinally collected in a neocortical focal epilepsy rat model. We measured classification accuracy in two supervised segmentation models: i.e. the generalized linear model and the nonlinear random forest model—by comparing computed white matter probabilities with actual neuroanatomically identified white matter. We found excellent overall discriminatory power for both models. However, the random forest model demonstrated a superior goodness-of-fit calibration plot that was close to the ideal calibration line. Based on this model, we measured that total white matter volume increased in young adult control and epileptic rats over a period of 10 weeks, but the average white matter volume was significantly lower in the focal epilepsy group. Changes in gray matter volume were not significantly different between control and epileptic rats. Our results (1) indicate that recurrent spontaneous seizures have an adverse effect on global white matter growth and (2) show that individual whole brain white matter volume can be accurately determined using a combination of multiparametric MRI and supervised segmentation models, offering a powerful tool to assess white matter volume changes in preclinical studies of neurological disease.

Keywords White matter · Gray matter · Focal epilepsy · Rat brain · Structural MRI · Supervised segmentation

Introduction

Focal epilepsy is one of the most common neurological diseases, with a prevalence of 0.4 % in high-income countries (Koepp and Woermann 2005). In up to one-third of patients, seizures are refractory to drug therapy (Kwan and Brodie 2000). MRI is commonly used to identify the pathological substrate of focal epilepsy (Duncan 1997). In the majority of patients with focal epilepsy, conventional MRI reveals structural pathology that is causally related to epilepsy, such as hippocampal sclerosis (Li et al. 1995; Jackson et al. 1990) and cortical dysgenesis (Sisodiya 2004). Nevertheless, in 20 % of individuals with refractory focal epilepsy, the MRI scan is "negative", that is, pathology is not found on visual inspection (Von Oertzen et al. 2002; Wiebe et al. 2001; Li et al. 1995).

More recently, new imaging techniques specifically tailored to quantify white matter volumes, have been applied in patients with focal epilepsy and negative

Electronic supplementary material The online version of this article (doi:10.1007/s00429-013-0633-4) contains supplementary material, which is available to authorized users.

W. M. Otte · K. P. J. Braun
Department of Pediatric Neurology, Rudolf Magnus Institute of Neuroscience, University Medical Center Utrecht, Utrecht, The Netherlands

W. M. Otte (✉) · M. P. A. van Meer · K. van der Marel · R. Zwartbol · M. A. Viergever · R. M. Dijkhuizen
Biomedical MR Imaging and Spectroscopy Group, Image Sciences Institute, University Medical Center Utrecht, Heidelberglaan 100, 3584 CX Utrecht, The Netherlands
e-mail: wmotte@gmail.com

conventional MRI findings and showed a reduction in total white matter volume (McMillan et al. 2004; Seidenberg et al. 2005; Bernasconi et al. 2004). In addition, diffusion tensor imaging, an MRI method that allows quantification of microstructural white matter integrity, has demonstrated significant white matter abnormalities throughout the brain: including the contralateral hemisphere—in patients with temporal lobe epilepsy (TLE) (Gross 2011; Otte et al. 2010, 2012b), suggesting that white matter is involved in the pathophysiological process of focal epilepsy. However, to determine whether white matter changes are the consequence of the seizure disorder, and not merely reflect an epiphenomenon that is related to the underlying cause of the epilepsy (the developmental or acquired epileptogenic pathology itself may involve white matter structures), more fundamental research is needed. This includes animal studies using well-controlled refractory focal epilepsy models combined with longitudinal MRI monitoring, starting after the onset of seizures or even in the subclinical stage of epileptogenesis.

To estimate white matter volumes from clinical MRI scans, multiple neuroimaging frameworks are available, e.g., the statistical parametric mapping (SPM) software (Ashburner and Friston 2005), FMRIB's software library (FSL) (Smith et al. 2004) and the free surfer image analysis suite (Dale et al. 1999). Volumetric information on different brain tissue classes is obtained after matching of individual patient brain scans with an average human brain template. Unfortunately, these frameworks cannot be straightforwardly applied to data from animal models (Uberti et al. 2009).

Supervised segmentation models that belong to the general machine learning-based pattern recognition techniques (Bishop 2006) provide a promising, yet unexplored, alternative to derive white matter volumes in a preclinical setting. A supervised segmentation model is able to assign white matter probabilities to brain voxels, which in turn allows calculation of brain white matter volumes. This assignment is based on voxel characteristics or features. Typically, combining multiple voxel features, e.g., from different image acquisitions with anatomical information on voxel location, increases model robustness (Bezdek et al. 1993). To assign probabilities to voxels, a model has to be 'trained' first on the basis of representative data. Such training data consist of multiple voxels with different features of which the correct tissue class (i.e., white matter) has been provided by one or more rat brain experts. After the training phase, the supervised segmentation model may be applied to new, unseen data. Supervised segmentation models do not require matching with a common template. They enable easy incorporation of multiple features to alleviate the bias imposed by basing classification decision on a single intensity value taken from the common templates white matter prior map. Despite the increase of preclinical MRI studies, to our knowledge, no supervised segmentation model has previously been applied in rodent epilepsy models. In this study, we developed two supervised segmentation models and tested their applicability in a multiparametric MRI dataset from epileptic rat brain.

In this study, we aimed to accurately characterize white matter volume changes over time in young adult rats with and without neocortical refractory focal epilepsy. To this aim, we determined if supervised segmentation models have sufficient accuracy to detect white matter volume changes in a preclinical setting with a minimal overall discriminatory power of 95 %. Based on previous clinical studies (McMillan et al. 2004; Seidenberg et al. 2005), we expected significantly reduced white matter volumes in rats with focal epilepsy, persisting over time. Accurate characterization of white matter volume changes may provide better insight into the yet unknown pathophysiological mechanism of remote cerebral white matter abnormalities in focal epilepsy.

Materials and methods

Animals

The animal experimental protocol was approved by the Utrecht University Ethical Committee on Animal Experiments. All experiments were carried out in accordance with the guidelines of the European Communities Council Directive. In total 26, 9-week-old adult male Sprague–Dawley rats (Charles River Laboratories International Inc., MA, USA) were included in this study. This age corresponds with late adolescence to early adulthood in humans (Brenhouse and Andersen 2011). Thirteen animals served as controls. Average weight of the animals at study inclusion was 283 ± 25 g. All animals were group-housed under standard, controlled conditions (food and water provided ad libitum, room temperature 22–24 °C, 12 h light/12 h dark cycle).

Focal neocortical epilepsy model

Chronic focal neocortical epilepsy was induced in 13 rats using the tetanus toxin model (Jefferys et al. 1995; Nilsen et al. 2005). Under anesthesia [subcutaneous injection of a mixture of 0.315 mg/mL fentanyl citrate and 10 mg/mL fluanisone (0.55 mL/kg, Hypnorm®, VetaPharm, Leeds, United Kingdom) and 50 mg/mL midazolam (0.55 mL/kg, Dormicum®, Roche Nederland B·V., Woerden, The Netherlands)], animals were stereotaxically injected in the right primary motor cortex (at 0.5 mm anterior and 2.5 mm lateral from bregma) using a 2.0-μL Hamilton syringe with

a 32G needle with 0.6 μL of tetanus toxin solution (100 ng/μL dissolved in 0.2 % bovine gelatin, Sigma–Aldrich, Zwijndrecht, The Netherlands). Based on visual inspection, all 13 rats developed spontaneous recurrent seizures after a latent period of 1 week. During follow-up, animals were monitored on a weekly basis and prior to scan sessions to detect behavioral changes reflecting clinical seizures. Seizure activity was defined as behavioral arrest with motor signs, including bilateral twitching of whiskers, bilateral facial twitching, and facial twitching together with bilateral myoclonic jerks of muscles around the skull and in the neck region (Jefferys et al. 1995; Nilsen et al. 2005, 2006).

Data collection

Multiparametric MRI was executed at 7, 21, 49, and 70 days after tetanus toxin injection. Rats were anaesthetized with 4 % isoflurane for endotracheal intubation, followed by mechanical ventilation (rate 52–59 min^{-1}; Columbus Instrument, Columbus, OH, USA) with 2.0 % isoflurane in air/O_2 (2:1) during MRI. MRI measurements were conducted on a 4.7 T horizontal bore MR system (Varian, Palo Alto, CA, USA) with a gradient-coil insert (125 mm internal diameter; 500 mT/m maximum gradient strength with 110 μs rise time) (Magnex Scientific, Oxford, UK). A Helmholtz volume coil (90 mm diameter) and an inductively coupled surface coil (25 mm diameter) were used for signal excitation and detection, respectively. Rats were placed in an MR-compatible stereotactic holder and immobilized with earplugs and a tooth-holder. During MRI, blood oxygen saturation and heart rate were continuously monitored by a pulse oximeter (8600V, Nonin Medical Inc., Plymouth, MN, USA) with the probe positioned on a hind paw. In addition, expired CO_2 was continuously monitored with a capnograph (Multinex 4200, Datascope Corp., Fairfield, NJ, USA), and body temperature was maintained at 37.0 ± 0.5 °C using a feedback-controlled heating pad. End-tidal CO_2 levels were kept within the normal range, equivalent to arterial pCO_2 levels between 35 and 45 mmHg (calculated from previous calibration measurements), by adjusting ventilation volume and/or rate.

The MRI acquisitions included multi-echo multi-slice T_2-weighted MRI [repetition time (TR)/echo time (TE) = 3,600/15 ms; echo train length = 12; 19 1 mm-coronal slices; field-of-view (FOV) = 32 × 32 mm^2; acquisition matrix = 256 × 128; voxel resolution = 0.125 × 0.25 × 1.0 mm^3] and diffusion tensor imaging (DTI) [four-shot spin-echo EPI; TR/TE = 3,500/26 ms; 25 0.5 mm axial slices; FOV = 32 × 32 mm^2; acquisition matrix = 64 × 64; voxel resolution = 0.5 × 0.5 × 0.5 mm^3; diffusion-weighting in 50 directions with b = 1,250 s/mm^2 (Δ/δ = 11/6 ms); 2 images without diffusion-weighting (b = 0)].

Image processing

Brain voxels were characterized using multiparametric features, based on DTI-based maps, T_2 maps and spatial maps. Specifically, the combination of spatial information and signal intensities is known to increase supervised segmentation robustness (Anbeek et al. 2004). First, diffusion-weighted images were corrected for motion and residual eddy current distortion by mutual information-based affine registration of all images to the baseline image (Pluim et al. 2003; Mangin et al. 2002). Next, the effective diffusion tensor, the corresponding eigensystem, and the subsequently derived fractional anisotropy (FA) and mean diffusivity (MD) were computed for each voxel (Basser and Pierpaoli 1996). Absolute T_2 values were calculated using nonlinear Levenberg–Marquardt fitting of the multi-echo T_2-weighted signal intensities. T_2 maps were matched with the DTI-based maps using within-subject affine registration followed by b-spline interpolation (elastix toolbox (Klein et al. 2010)). Spatial maps included the maps for the x-, y- and z-coordinates and Euclidean distance transform to the brain surface (Danielsson 1980). Spatial maps may potentially contain strong discriminating information to separate white matter from non-white matter voxels (e.g., white matter never 'touches' brain edges, whereas gray matter does). The brain surface was determined using a deformable surface model that works well for human as well as rodent brain MRI images (Smith 2002).

Manual white matter delineation

A biotechnician trained in rat brain anatomy (R.Z.) was presented with the T_2-weighted images, absolute T_2 and DTI-based maps from 20 randomly selected control MRI datasets to manually outline cerebral white matter voxels in the brain, excluding the cerebellum and brain stem (Suppl. Fig. 1). This was considered as the reference dataset. A second author (W.M.O) delineated a subset of these datasets as well. Between-observer agreement was tested with the Cohen's kappa coefficient, which is a commonly used statistical measure of inter-rater agreement (Carletta 1996). The observed coefficient was >0.7, indicating a 'good' (Fleiss 1981) or 'substantial agreement' between both observers (Landis and Koch 1977). The T_2-weighted images were primarily used to delineate the white matter structures and to serve as reference for the other images on which the white matter border was uncertain. Delineated white matter structures included: (1) anterior commissure, (2) cerebral peduncle, (3) cingulum, (4) commissural stria terminalis, (5) commissure of the inferior colliculus, (6) commissure of the lateral lemniscus, (7) commissure of the superior colliculus, (8) corpus callosum (including genu and rostrum), (9) cuneate fasciculus, (10) dorsal

corticospinal tract, (11) dorsal tegmental bundle, (12) external capsule, (13) external medullary lamina, (14) fimbria of the hippocampus, (15) forceps minor and major of the corpus callosum, (16) hippocampal fissure, (17) internal arcuate fibers, (18) internal capsule, (19) medial forebrain bundle, (20) medial longitudinal fasciculus, (21) pyramidal tract, and (22) superior thalamic radiation, based on the Paxinos and Watson (2007) rat brain atlas.

The manually delineated white matter volume was 160 ± 22 mm^3 [mean standard $\pm$ deviation (SD)]. The total brain volume, including gray matter and cerebrospinal fluid, was $2{,}481 \pm 144$ mm^3. Using all voxels in the model training would lead to a highly unbalanced dataset with <10 % of the voxels being labeled as white matter. Therefore, we did not present all non-white matter voxels to the models, but randomly selected a similar amount (i.e., approximately 160 mm^3) of non-white matter voxels in each dataset.

Supervised segmentation models

Generalized linear and random forest model training and evaluation were done in the open-source *R* (Ihaka and Gentleman 1996) software using the *rattle* (Williams 2009) package.

As preprocessing, white matter voxels were labeled as 1 and non-white matter voxels as 0. Because multilevel supervised segmentation models are relatively difficult to design and we do not expect better performance with a 3-class segmentation model in classifying white matter volumes, we did not separate gray matter from cerebrospinal fluid (CSF). By combining all non-white matter voxels in a single class, we were able to model white matter as a dichotomous dependent variable. Details on the segmentation models and their performance are provided as Supplementary data.

Volume measurements

After training and evaluation of the GLM and random forest models, we selected the best performing model, in terms of discriminatory power, and applied this model to all datasets in both the control and focal epilepsy groups. Total and relative white matter volumes were calculated from white matter probabilities assigned to all brain voxels. We did not round the probabilities to 0 or 1, as this leads to information loss. Instead, we summed all voxel volumes multiplied by their white matter probability.

To measure the gray matter volume, we first determined which voxels represented CSF on T_2 maps (all voxels with a T_2 value >0.1 s within the brain mask were labeled as CSF). Gray matter volume was subsequently calculated as total brain volume minus CSF volume minus white matter volume.

Finally, we analyzed the absolute and relative volumes of white matter, gray matter and CSF using linear mixed modeling (*R* package *nlme*) with group (i.e., control or epilepsy), time (i.e., day 7, 21, 49, or 70) and group $\times$ time interaction as factors, while correcting for repeated measures within rats (Pinheiro and Bates 2000). Potential temporal correlations within rats were corrected with an autocorrelation structure of order 1 (AR1), with a continuous time covariate (Pinheiro and Bates 2000). A similar linear mixed model was used for analysis of body weight, starting at time-point day 0. Regression analysis between absolute volumes (gray and white matter) and body weights was performed using additional linear mixed models with AR1 correction. Subsequently, we did linear mixed model regression analysis between absolute and relative white matter volumes and average FA and MD for all voxels with a white matter probability >50 %.

All values are presented as mean $\pm$ SD. $p < 0.05$ was considered significant.

Results

Animal model

All rats injected with tetanus toxin developed epilepsy after a latent period of 1 week, characterized by spontaneous, frequent, and well-tolerated seizures similar to previous descriptions of this model (Louis et al. 1990; Brener et al. 1991; Nilsen et al. 2005, 2006; Otte et al. 2010, 2012a, b). All rats continued to have seizures during the entire time frame of the study. Four rats developed a status epilepticus in the first 2 weeks after tetanus toxin injection and were excluded.

Body weight increased from 274.6 ± 6.2 and 285.9 ± 28.8 g at day 0 to 511.2 ± 48.6 and 525.8 ± 44.2 g at day 70 in the control and epilepsy group, respectively. No group effect was found, but a group $\times$ time interaction was present at 21 days with body weight being lower in the epilepsy group as compared to controls (-53.5 ± 15.3 g, $p = 0.0004$).

MRI

No brain abnormalities were detected by visual inspection of the T_2-weighted images, T_2 maps, and DTI maps in the control and epilepsy rats, and brain images appeared similar between the two groups.

Model performance

The discriminatory power of the GLM and random forest model to segment white matter was excellent (Suppl.

Fig. 2a, b, respectively); however, the random forest model clearly provided better probability maps than the GLM. The latter suffers from false positive probabilities (i.e., non-white matter voxels labeled as white matter) assigned to cortical, subcortical and extra cerebral areas. Similar patterns were found for the other rat datasets.

Based on these findings, we decided to use the random forest model as our preferred supervised segmentation model to calculate and compare white matter volumes between control and epileptic rats.

Volume measurements

Total brain volume over time is plotted in Fig. 1a. Total brain volume was significantly smaller in epileptic rats at day 7 as compared to controls (-0.16 ± 0.05 cm^3, $p = 0.0084$). A significant total brain volume increase between days 7 and 70 was found in the control group (0.10 ± 0.02 cm^3, $p < 0.0001$) and in the epilepsy group (0.14 ± 0.03 cm^3, $p < 0.0001$).

The CSF volume change over time for both groups is presented in Fig. 1b. CSF volume had significantly increased at days 49 (control 37.3 ± 9.5 mm^3, $p = 0.0002$; epilepsy 41.6 ± 12.3 mm^3, $p = 0.0012$) and 70 (control 68.8 ± 9.6 mm^3, $p < 0.0001$; epilepsy 75.8 ± 12.4 mm^3, $p < 0.0001$) as compared to day 7. There was no group effect or group × time interaction.

White matter volumes for the control and epileptic rats were determined with the final random forest model at days 7, 21, 49 and 70 (Fig. 2a). The total white matter significantly increased over time in the control (0.75 ± 0.06 mm^3/day, $p < 0.0001$) and focal epilepsy groups (0.50 ± 0.07 mm^3, $p < 0.0001$). The average white matter volume in controls during the total study period was 213.8 ± 3.5 mm^3. In the focal epilepsy group, white matter volume was on average reduced by -18.8 ± 6.9 mm^3 relative to the controls ($p = 0.0002$). The interaction term group × time was not significant ($p = 0.10$). Cross-sectionally, a significant lower white matter volume (-16.3 ± 6.9 mm^3) was found in the epilepsy group at day 70 ($p = 0.020$). White matter volume correlated positively with body weight in the control ($r = 0.71 \pm 0.14$, $p < 0.0001$) and epilepsy group ($r = 0.74 \pm 0.20$, $p = 0.001$).

As total brain size could potentially bias our absolute white matter volume data, we also statistically tested the relative white matter volumes (Fig. 2b). Similar patterns of growth over time as well as differences between the control and focal epilepsy rats were found. The relative white matter increase over time was 0.025 ± 0.002 %/day ($p < 0.0001$) for the controls and 0.015 ± 0.003 %/day ($p < 0.0001$) for the focal epilepsy rats. The epilepsy group had a relative white matter volume that was reduced by 0.33 ± 0.22 % ($p = 0.0013$) as compared with controls. The interaction term group × time was not significant ($p = 0.09$).

Absolute and relative white matter volume correlated positively with the average FA in the control group (absolute: $r = 0.29 \pm 0.12$, $p = 0.015$; relative: $r = 0.23 \pm 0.10$, $p = 0.03$), and the epilepsy group (absolute: $r = 0.56 \pm 0.16$, $p = 0.0008$; relative: $r = 0.54 \pm 0.18$, $p = 0.004$).

Negative correlations were found between white matter volume and MD in the control group (absolute: not significant; relative: $r = -0.22 \pm 0.10$, $p = 0.04$), and the

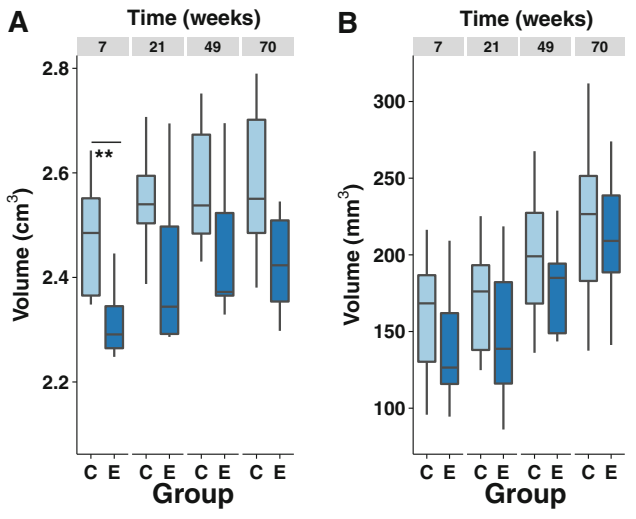

Fig. 1 **a** Box plots of serial total brain volume (cerebrospinal fluid, white matter and gray matter) in controls (C) and rats with focal epilepsy (E) at days 7, 21, 47 and 70. **b** Box plots of serial cerebrospinal fluid volume. $^{**}p < 0.01$

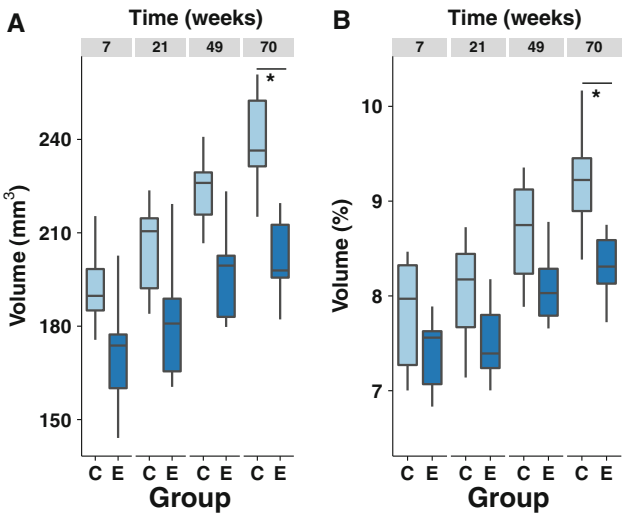

Fig. 2 **a** Box plots of white matter volume in controls (C) and rats with focal epilepsy (E) at days 7, 21, 47 and 70. **b** Box plots of white matter volume relative to total brain volume. This corrects for total brain volume as a potential confounder for white matter volume differences between control and epileptic rats. $^{*}p < 0.05$

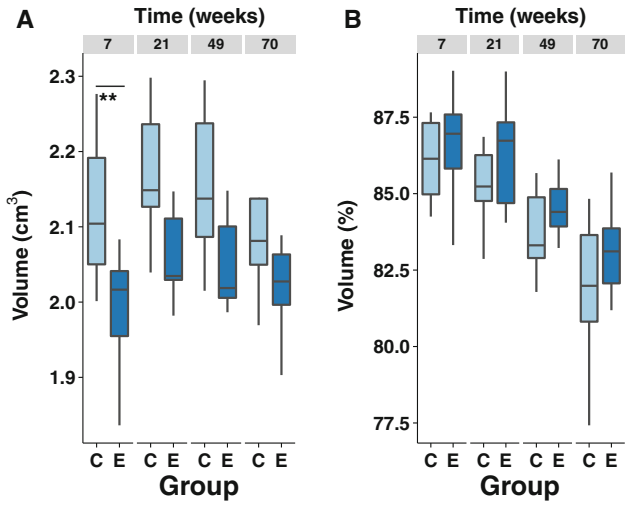

Fig. 3 **a** Box plots of gray matter volume in controls (C) and rats with focal epilepsy (E) at day 7, 21, 49 and 70. **b** Box plots of gray matter volume relative to total brain volume. $^{**}p < 0.01$

epilepsy group (absolute: $r = -0.57 \pm 0.16$, $p = 0.001$; relative: $r = -0.55 \pm 0.18$, $p = 0.003$).

Gray matter volumes are shown in Fig. 3a. A group × time interaction was found at day 7 (-0.12 ± 0.04 cm^3, $p = 0.009$). Gray matter volume was significantly higher after 21 days in the control group as compared to day 7 (0.05 ± 0.02 cm^3, $p = 0.02$). No significant changes in gray volume were found in the epilepsy group. A significant negative correlation was found between gray matter volume and body weight in the control group ($r = -0.48 \pm 0.18$, $p = 0.01$), but not in the epilepsy group.

Relative gray matter volumes decreased over time in both groups (Fig. 3b), but differences with day 7 were only significant for the control group at day 49 (-2.24 ± 0.33 %, $p < 0.0001$) and day 70 (-4.03 ± 0.35 %, $p < 0.0001$). No group effect or group × time interaction was found.

Discussion

Focal epilepsy is increasingly being recognized as both a gray and white matter disease (Otte et al. 2012b; Gross 2011; Salmenpera and Duncan 2005; McMillan et al. 2004; Seidenberg et al. 2005; Vaessen et al. 2011). Nevertheless, how and to what extent focal epilepsy affects the global brain white matter is largely unknown. In addition, white matter pathology remains poorly characterized and its underlying pathophysiological mechanisms are incompletely understood. In this study, we aimed to elucidate the relationship between focal epilepsy and white matter volume over time, in a rat model of refractory neocortical focal epilepsy. We showed that individual whole brain white matter probability maps can be accurately determined using a combination of multiparametric MRI and a random forest supervised segmentation model.

Normal brain development

Our observed gray and white matter volume changes, occurring during late adolescence and early adulthood in control rats, are in line with earlier studies. It has been shown that gray matter volume temporally follows an inverted U-shape pattern, whereas white matter density and volume continue to increase (Brummelte and Teuchert-Noodt 2006; Brenhouse et al. 2008; Cunningham et al. 2002; Brenhouse and Andersen 2011). The pattern of absolute gray matter volumes in our study indeed resembles an inverted U-shape (Fig. 3a), with a maximum gray matter volume between 12 and 16 weeks of age, while white matter volume kept growing. Possible explanations for the later reduction in gray matter volume may include a halt of synaptic overproduction during late adolescence, which would change the synaptic density, and extensive pruning with significant loss of cortical neurons (Markham et al. 2007). Synaptic, neuronal and axonal pruning is an essential step during brain development, starting early after birth and completed around the time of sexual maturation [for review see: (Luo and O'Leary 2005)] and has been found in rats (Andersen and Teicher 2004) as well as in humans (Glantz et al. 2007). Failure to prune excessive excitatory synapses during development has been linked to epileptogenesis in a C1q knockout mice model (Chu et al. 2010), but it is unknown whether a pruning dysregulation plays a role in the tetanus toxin epilepsy model.

The absolute and relative white matter volumes in the control group of our study showed a progressive linear growth (Fig. 2). Much of the developmental white matter volume increase is known to be due to myelination of neuronal fibers (Benes et al. 1994). Ongoing myelination, continuing during early adulthood, has been observed in the corpus callosum (Rajapakse et al. 1996), internal capsule and the fasciculus arcuatus (Brenhouse and Andersen 2011; Paus 2005, 2010).

Focal epilepsy

White matter growth lagged behind in rats with focal epilepsy and we detected a significant reduction in white matter volume after 10 weeks of active epilepsy (Fig. 2). A difference in absolute gray matter volume was found between epilepsy and control groups at day 7 only (Fig. 3). Relative gray matter volumes were not different between groups.

The observed relative reduction of white matter volume in experimental focal epilepsy is in line with clinical

studies on white matter volumes in TLE. Cross-sectionally, ipsilateral and contralateral white matter loss was found with MRI in 34 patients suffering from unilateral left temporal lobe epilepsy, as compared with 65 controls (Seidenberg et al. 2005). In that study, duration of epilepsy was associated with a reduced ipsilateral white matter volume, and age at recurrent seizures was associated with white matter volume asymmetry between hemispheres. Gray matter volume was not significantly affected. These results are in agreement with our relative white matter volume data (Fig. 3b), where we corrected for volume changes in non-white matter. Another clinical cross-sectional TLE study has reported changes in white matter volume as compared with controls (Hermann et al. 2003b). Total white matter was reduced with 9.8 %, whereas gray matter and total cerebral volumes decreased to a lesser extent, 3.0 and 5.8 %, respectively. Yet another study in unilateral TLE has addressed white matter volume changes using voxel-based morphometry (McMillan et al. 2004) and found wide-spread white matter abnormalities in temporal and extratemporal lobes. Finally, support for loss of white matter in focal epilepsy has been provided by a study on the corpus callosum in patients with chronic TLE (Hermann et al. 2003a). The volume of the corpus callosum was smaller as compared with controls.

Important information that our study adds to the findings from cross-sectional clinical studies in TLE is that (1) white matter volume changes are not only restricted to TLE, but also appear in extratemporal neocortical epilepsy; (2) the relatively smaller volume emerges early, is persistent over time and may even progress; (3) the changes in white matter volume cannot be explained by other factors that may contribute to the white matter pathology found in clinical study populations, such as the underlying epileptogenic pathology, early neurodevelopmental disruptions, chronic use of antiepileptic drugs, or the early brain insult: e.g., infantile status epilepticus or prolonged febrile seizures—that often precedes the epileptogenic process in patients with TLE. In our study, normal animals were used in which epilepsy was induced during late adolescence, without prior status epilepticus, and unaccompanied by treatment with antiepileptic drugs. Since the intracortical injection of tetanus itself does not cause significant microstructural tissue damage (Barkmeier and Loeb 2009), we propose that white matter pathology in this model can be at least partially attributed to the repeated seizures or an interaction between normal myelination of white matter fibers and repeated seizures. Nonetheless, this hypothesis remains to be confirmed in studies that will include more (earlier) time points and focus on distinct periods within the neurodevelopmental time frame including adolescence and late adulthood. Interactions between white matter changes and epilepsy may be different across lifespan as myelin deposition (Norton and Poduslo 1973) and white matter volume (van der Marel et al. 2013) continues to increase far into adulthood, and cerebral structures may consequently respond differently to recurrent seizures.

The method we used to determine white matter volumes in rat brains differs from the standard software procedures utilized in clinical settings which critically depend on nonlinear matching with a human template image (Ashburner and Friston 2005; Smith et al. 2004; Dale et al. 1999). A first attempt to use rat brain template matching in estimating brain white matter volume has recently resulted in an SPM software extension (Valdés-Hernández et al. 2011). This approach may very well serve as an alternative for the supervised segmentation approach we used in our study. However, it requires a 3D T_2-weighted scan to match with the rat brain template. Valdés-Hernández et al. 2011 found, based on histogram analysis, 64 % (1,111 $\pm$ 44 mm^3) of the rat brain to be white matter. This is substantially larger than the 8–10 % white matter volume we found (Fig. 2b). There are several explanations for the apparent discrepancy in reported white matter volumes. First, large subcortical structures, which include the thalamus and colliculi, are conventionally considered gray matter, although their T_2-weighted voxel intensities are within the normal white matter range. Therefore, the authors' intensity-based unsupervised clustering algorithm incorrectly assigned high white matter probabilities to these structures, whereas our supervised classification approach enables more stringent adherence to labeling of the Paxinos and Watson (2007) rat brain atlas. Second, differences in findings may also be related to more partial volume effects in our multislice MR data with higher slice thicknesses, which could have blurred white matter voxels towards gray matter. Nevertheless, it has been shown from histological examinations that the total white matter volume in 6–8 months old adult rats is 119 mm^3 on average (Li et al. 2008). We measured average white matter volumes of 213.8 $\pm$ 3.50 mm^3 in control rats in a time range of 9–19 weeks. This indicates that our random forest model white matter probability maps and derived white matter volumes (Fig. 2) are in close agreement with the earlier histological findings (Li et al. 2008). The overestimation is probably due to the earlier mentioned partial volume effects in our data.

Supervised segmentation to determine white matter volume has not previously been applied to rodent brain. As MRI is becoming an increasingly popular tool for in vivo studies in epilepsy rat models [for reviews see (Grohn et al. 2011; Obenaus and Jacobs 2007)], as well as other rodent models of neurological diseases [for reviews see (Anderson and Frank 2007; Dijkhuizen 2006)], this new volumetric approach provides excellent opportunities to accurately determine in vivo white matter volumes in rodent brain

studies. In a clinical setting a supervised segmentation model, based on the so-called support vector machine method, has recently been successfully applied to automatically and accurately classify tissue based on T_2 and DTI images of TLE patients (Focke et al. 2012). This underscores the potential of supervised segmentation to determine white matter volumes both in clinical and preclinical settings.

The exact mechanism behind the reduced white matter volume in clinical and experimental epilepsy remains to be determined. It is most likely to be multifactorial. Two studies have indicated that normal myelination is hampered in nearby and remote white matter (van Eijsden et al. 2011; Concha et al. 2010). Others studies have provided evidence that focal epilepsy is a large brain network disease [for review see (Stam and van Straaten 2012)]. Interestingly, a recent study that applied structural whole brain network analysis to individuals with chronic TLE revealed impaired white matter networks, while white matter volume was preserved (Vaessen et al. 2011). Evidently, more research is needed to elucidate how focal epilepsy affects white matter in general and its volume in particular. Based on our current findings, we speculate that white matter volume changes may be related to normal white matter development interacting with frequent seizure propagation in large epileptic networks that include white matter, which would particularly affect axonal myelination and formation of axonal spines. The latter is based on results from hippocampal studies that showed adverse effects due to prolonged seizure activity, including axonal demyelination, formation of axonal spines, increase in interstitial fluid volume due to edema, replacement of axons by glial cells, and astrocytic proliferation [for review see (Sutula et al. 2003)]. Indeed, white matter structures in the direct pathway of recurrent TLE seizures, i.e., the fimbriae and fornices, have been characterized with increased extra-axonal fraction, reduced axonal membrane circumference and myelin area in a post-surgical histological analysis (Concha et al. 2010). Wallerian degeneration has also been suggested as a mechanism of seizure-induced white matter damage, although direct evidence is not available (Kim et al. 2008).

Conclusions

In summary, our study demonstrates that supervised segmentation methods are equally promising in experimental settings as they are in clinical settings, and offer powerful tools for in vivo assessment of white matter changes. This provides potential opportunities for imaging studies that look into the role of white matter in neurodevelopmental and neurological disorders, including epilepsy, stroke, Alzheimer's disease and multiple sclerosis. We showed that, compared to age-matched control animals, there is less increase of white matter volume over time in experimental focal epilepsy that is induced in rats with neither underlying neurodevelopmental disorder nor antiepileptic treatment. This strongly suggests that ongoing seizures affect normal maturation of white matter. Our findings support further studies on the role of the brain's white matter in recurrent spontaneous seizures.

Acknowledgments This research was supported by the Dutch National Epilepsy Fund (NEF nr. 08-10) and Utrecht University's High Potential program. The funders had no role in study design, data collection and analysis, decision to publish, or preparation of the manuscript.

References

Anbeek P, Vincken KL, van Osch MJ, Bisschops RH, van der Grond J (2004) Probabilistic segmentation of white matter lesions in MR imaging. Neuroimage 21(3):1037–1044

Andersen SL, Teicher MH (2004) Delayed effects of early stress on hippocampal development. Neuropsychopharmacology 29(11):1988–1993

Anderson SA, Frank JA (2007) MRI of mouse models of neurological disorders. NMR Biomed 20(3):200–215

Ashburner J, Friston KJ (2005) Unified segmentation. Neuroimage 26(3):839–851

Barkmeier DT, Loeb JA (2009) An animal model to study the clinical significance of interictal spiking. Clin EEG Neurosci 40(4): 234–238

Basser PJ, Pierpaoli C (1996) Microstructural and physiological features of tissues elucidated by quantitative-diffusion-tensor MRI. J Magn Reson B 111(3):209–219

Benes FM, Turtle M, Khan Y, Farol P (1994) Myelination of a key relay zone in the hippocampal formation occurs in the human brain during childhood, adolescence, and adulthood. Arch Gen Psychiatry 51(6):477–484

Bernasconi N, Duchesne S, Janke A, Lerch J, Collins DL, Bernasconi A (2004) Whole-brain voxel-based statistical analysis of gray matter and white matter in temporal lobe epilepsy. Neuroimage 23(2):717–723

Bezdek JC, Hall LO, Clarke LP (1993) Review of MR image segmentation techniques using pattern recognition. Med Phys 20(4):1033–1048

Bishop CM (2006) Pattern recognition and machine learning, vol 4. SpringerLink, New York

Brener K, Amitai Y, Jefferys JG, Gutnick MJ (1991) Chronic epileptic foci in neocortex: in vivo and in vitro effects of tetanus toxin. Eur J Neurosci 3(1):47–54

Brenhouse HC, Andersen SL (2011) Developmental trajectories during adolescence in males and females: a cross-species understanding of underlying brain changes. Neurosci Biobehav Rev 35(8):1687–1703

Brenhouse HC, Sonntag KC, Andersen SL (2008) Transient D1 dopamine receptor expression on prefrontal cortex projection neurons: relationship to enhanced motivational salience of drug cues in adolescence. J Neurosci 28(10):2375–2382

Brummelte S, Teuchert-Noodt G (2006) Postnatal development of dopamine innervation in the amygdala and the ento rhinal cortex of the gerbil (*Meriones unguiculatus*). Brain Res 1125(1):9–16

Carletta J (1996) Assessing agreement on classification tasks: the kappa statistic. Comput Linguist 22(2):249–254
Chu Y, Jin X, Parada I, Pesic A, Stevens B, Barres B, Prince DA (2010) Enhanced synaptic connectivity and epilepsy in C1q knockout mice. Proc Natl Acad Sci USA 107(17):7975–7980
Concha L, Livy DJ, Beaulieu C, Wheatley BM, Gross DW (2010) In vivo diffusion tensor imaging and histopathology of the fimbria-fornix in temporal lobe epilepsy. J Neurosci 30(3):996–1002
Cunningham MG, Bhattacharyya S, Benes FM (2002) Amygdalocortical sprouting continues into early adulthood: implications for the development of normal and abnormal function during adolescence. J Comp Neurol 453(2):116–130
Dale AM, Fischl B, Sereno MI (1999) Cortical surface-based analysis. I. Segmentation and surface reconstruction. Neuroimage 9(2):179–194
Danielsson PE (1980) Euclidean distance mapping. Comput Graph Image Process 14:227–248
Dijkhuizen RM (2006) Application of magnetic resonance imaging to study pathophysiology in brain disease models. Methods Mol Med 124:251–278
Duncan JS (1997) Imaging and epilepsy. Brain 120(Pt 2):339–377
Fleiss JL (1981) The measurement of interrater agreement. Stat Med Rates Proportions 2:212–236
Focke NK, Yogarajah M, Symms MR, Gruber O, Paulus W, Duncan JS (2012) Automated MR image classification in temporal lobe epilepsy. Neuroimage 59(1):356–362
Glantz LA, Gilmore JH, Hamer RM, Lieberman JA, Jarskog LF (2007) Synaptophysin and postsynaptic density protein 95 in the human prefrontal cortex from mid-gestation into early adulthood. Neuroscience 149(3):582–591
Grohn O, Sierra A, Immonen R, Laitinen T, Lehtimaki K, Airaksinen A, Hayward N, Nairismagi J, Lehto L, Pitkanen A (2011) Multimodal MRI assessment of damage and plasticity caused by status epilepticus in the rat brain. Epilepsia 52(Suppl 8):57–60
Gross DW (2011) Diffusion tensor imaging in temporal lobe epilepsy. Epilepsia 52(Suppl 4):32–34
Hermann B, Hansen R, Seidenberg M, Magnotta V, O'Leary D (2003a) Neurodevelopmental vulnerability of the corpus callosum to childhood onset localization-related epilepsy. Neuroimage 18(2):284–292
Hermann B, Seidenberg M, Bell B, Rutecki P, Sheth RD, Wendt G, O'Leary D, Magnotta V (2003b) Extratemporal quantitative MR volumetric and neuropsychological status in temporal lobe epilepsy. J Int Neuropsychol Soc 9(3):353–362
Ihaka R, Gentleman R (1996) R: a language for data analysis and graphics. J Comput Graph Stat 5(3):299–314
Jackson GD, Berkovic SF, Tress BM, Kalnins RM, Fabinyi GC, Bladin PF (1990) Hippocampal sclerosis can be reliably detected by magnetic resonance imaging. Neurology 40(12):1869–1875
Jefferys JGR, Borck C, Mellanby J (1995) Chronic focal epilepsy induced by intracerebral tetanus toxin. Ital J Neurol Sci 16(1):27–32
Kim H, Piao Z, Liu P, Bingaman W, Diehl B (2008) Secondary white matter degeneration of the corpus callosum in patients with intractable temporal lobe epilepsy: a diffusion tensor imaging study. Epilepsy Res 81(2–3):136–142
Klein S, Staring M, Murphy K, Viergever MA, Pluim JP (2010) Elastix: a toolbox for intensity-based medical image registration. IEEE Trans Med Imaging 29(1):196–205
Koepp MJ, Woermann FG (2005) Imaging structure and function in refractory focal epilepsy. Lancet Neurol 4(1):42–53
Kwan P, Brodie MJ (2000) Early identification of refractory epilepsy. N Engl J Med 342(5):314–319
Landis JR, Koch GG (1977) The measurement of observer agreement for categorical data. Biometrics 33(1):159–174
Li LM, Fish DR, Sisodiya SM, Shorvon SD, Alsanjari N, Stevens JM (1995) High resolution magnetic resonance imaging in adults with partial or secondary generalised epilepsy attending a tertiary referral unit. J Neurol Neurosurg Psychiatry 59(4):384–387
Li C, Yang S, Zhang W, Shi X, Wang W, Nyengaard JR, Tang Y (2008) Unbiased stereological quantification of unmyelinated fibers in the rat brain white matter. Neurosci Lett 437(1):38–41
Louis ED, Williamson PD, Darcey TM (1990) Chronic focal epilepsy induced by microinjection of tetanus toxin into the cat motor cortex. Electroencephalogr Clin Neurophysiol 75(6):548–557
Luo L, O'Leary DD (2005) Axon retraction and degeneration in development and disease. Annu Rev Neurosci 28:127–156
Mangin JF, Poupon C, Clark C, Le Bihan D, Bloch I (2002) Distortion correction and robust tensor estimation for MR diffusion imaging. Med Image Anal 6(3):191–198
Markham JA, Morris JR, Juraska JM (2007) Neuron number decreases in the rat ventral, but not dorsal, medial prefrontal cortex between adolescence and adulthood. Neuroscience 144(3):961–968
McMillan AB, Hermann BP, Johnson SC, Hansen RR, Seidenberg M, Meyerand ME (2004) Voxel-based morphometry of unilateral temporal lobe epilepsy reveals abnormalities in cerebral white matter. Neuroimage 23(1):167–174
Nilsen KE, Walker MC, Cock HR (2005) Characterization of the tetanus toxin model of refractory focal neocortical epilepsy in the rat. Epilepsia 46(2):179–187
Nilsen KE, Kelso AR, Cock HR (2006) Antiepileptic effect of gap-junction blockers in a rat model of refractory focal cortical epilepsy. Epilepsia 47(7):1169–1175
Norton WT, Poduslo SE (1973) Myelination in rat brain: changes in myelin composition during brain maturation. J Neurochem 21(4):759–773
Obenaus A, Jacobs RE (2007) Magnetic resonance imaging of functional anatomy: use for small animal epilepsy models. Epilepsia 48(Suppl 4):11–17
Otte WM, Dijkhuizen RM, Stam CJ, van der Marel K, van Meer MPA, Viergever MA, Braun KPJ (2010) Spatiotemporal network alterations in experimental focal cortical epilepsy: MRI-based longitudinal functional connectivity and weighted graph analysis. In: ISBI, IEEE, pp 888–891
Otte WM, Dijkhuizen RM, van Meer MP, van der Hel WS, Verlinde SA, van Nieuwenhuizen O, Viergever MA, Stam CJ, Braun KP (2012a) Characterization of functional and structural integrity in experimental focal epilepsy: reduced network efficiency coincides with white matter changes. PLoS ONE 7(7):e39078
Otte WM, van Eijsden P, Sander JW, Duncan JS, Dijkhuizen RM, Braun KP (2012b) A meta-analysis of white matter changes in temporal lobe epilepsy as studied with diffusion tensor imaging. Epilepsia 53:659–667
Paus T (2005) Mapping brain maturation and cognitive development during adolescence. Trends Cogn Sci 9(2):60–68
Paus T (2010) Growth of white matter in the adolescent brain: myelin or axon? Brain Cogn 72(1):26–35
Paxinos G, Watson C (2007) The rat brain in stereotaxic coordinates: hard cover edition. Academic press, San Diego
Pinheiro JC, Bates DM (2000) Mixed-effects models in S and S-PLUS. Springer Verlag, Berlin
Pluim JP, Maintz JB, Viergever MA (2003) Mutual-information-based registration of medical images: a survey. IEEE Trans Med Imaging 22(8):986–1004
Rajapakse JC, Giedd JN, Rumsey JM, Vaituzis AC, Hamburger SD, Rapoport JL (1996) Regional MRI measurements of the corpus callosum: a methodological and developmental study. Brain Dev 18(5):379–388
Salmenpera TM, Duncan JS (2005) Imaging in epilepsy. J Neurol Neurosurg Psychiatry 76(Suppl 3):iii2–iii10

Seidenberg M, Kelly KG, Parrish J, Geary E, Dow C, Rutecki P, Hermann B (2005) Ipsilateral and contralateral MRI volumetric abnormalities in chronic unilateral temporal lobe epilepsy and their clinical correlates. Epilepsia 46(3):420–430

Sisodiya SM (2004) Malformations of cortical development: burdens and insights from important causes of human epilepsy. Lancet Neurol 3(1):29–38

Smith SM (2002) Fast robust automated brain extraction. Hum Brain Mapp 17(3):143–155

Smith SM, Jenkinson M, Woolrich MW, Beckmann CF, Behrens TE, Johansen-Berg H, Bannister PR, De Luca M, Drobnjak I, Flitney DE, Niazy RK, Saunders J, Vickers J, Zhang Y, De Stefano N, Brady JM, Matthews PM (2004) Advances in functional and structural MR image analysis and implementation as FSL. Neuroimage 23(Suppl 1):S208–S219

Stam CJ, van Straaten EC (2012) The organization of physiological brain networks. Clin Neurophysiol 123(6):1067–1087

Sutula TP, Hagen J, Pitkanen A (2003) Do epileptic seizures damage the brain? Curr Opin Neurol 16(2):189–195

Uberti MG, Boska MD, Liu Y (2009) A semi-automatic image segmentation method for extraction of brain volume from in vivo mouse head magnetic resonance imaging using constraint level sets. J Neurosci Methods 179(2):338–344

Vaessen MJ, Jansen JF, Vlooswijk MC, Hofman PA, Majoie HJ, Aldenkamp AP, Backes WH (2011) White matter network abnormalities are associated with cognitive decline in chronic epilepsy. Cereb Cortex 22(9):2139–2147

Valdés-Hernández PA, Sumiyoshi A, Nonaka H, Haga R, Aubert-Vásquez E, Ogawa T, Iturria-Medina Y, Riera JJ, Kawashima R (2011) An in vivo MRI template set for morphometry, tissue segmentation, and fMRI localization in rats. Front Neuroinform 5:26

van der Marel K, Otte WM, Rudrapatna US, van der Toorn A, Dijkhuizen RM (2013) Longitudinal diffusion kurtosis imaging of normal white matter development in rats. In: BRAIN Conference, Translational Neuroscience From Molecules to Man, Shanghai

van Eijsden P, Otte WM, van der Hel WS, van Nieuwenhuizen O, Dijkhuizen RM, de Graaf RA, Braun KP (2011) In vivo diffusion tensor imaging and ex vivo histologic characterization of white matter pathology in a post-status epilepticus model of temporal lobe epilepsy. Epilepsia 52(4):841–845

Von Oertzen J, Urbach H, Jungbluth S, Kurthen M, Reuber M, Fernandez G, Elger CE (2002) Standard magnetic resonance imaging is inadequate for patients with refractory focal epilepsy. J Neurol Neurosurg Psychiatry 73(6):643–647

Wiebe S, Blume WT, Girvin JP, Eliasziw M (2001) A randomized, controlled trial of surgery for temporal-lobe epilepsy. N Engl J Med 345(5):311–318

Williams GJ (2009) Rattle: a data mining GUI for R. R J 1(2):45–55